Diyala Journal of Engineering Sciences

Journal homepage: https://djes.info/index.php/djes

ISSN: 1999-8716 (Print); 2616-6909 (Online)

Green Synthesis, Characterization and Evaluation of Biological Activities of Ag-Mno Nanocomposites from Cyttaranthus Congolensis

Giresse N. Kasiama[1*], Carlos N. Kabengele[1], Jason T. Kilembe[1], Jules M. Kitadi[3], Michel Mifundu[1], Jean Paul Ngbolua[2], Damien S.T. Tshibangu[1], Dorothée D. Tshilanda[1] and Pius T. Tshimankinda[1]

1 Department of Chemistry, Faculty of Sciences, University of Kinshasa, BP 190, Kinshasa XI, Democratic Republic of Congo.

2 Department of Biology, Faculty of Sciences, University of Kinshasa, BP 190, Kinshasa XI, Democratic Republic of Congo

3 Faculty of Sciences, University of Kikwit, BP76, Kikwit, Democratic Republic of Congo.

ARTICLE INFO

Article history:
Received May 3, 2023
Revised July 11, 2023
Accepted July 13, 2023
Available online September 1, 2023

Keywords:
Cyttaranthus congolensis
Silver
Manganese nanocomposites

ABSTRACT

This study conducts biogenic synthesis of Ag-MnO nanocomposites whose aqueous extract from *Cyttaranthus congolensis* was used as a reducer and stabiliser. The characterisation of these particles by UV–visible spectroscopy made it possible to identify the band linked to the surface plasmon resonance located at approximately 380 nm. X-ray diffraction and fluorescence allowed determining the presence of particles of formula Ag 0.21 Mn 0.28 O having crystallised in a monoclinic system (a= 5.8517 Å, b = 3.4674 Å, c = 5.4838 Å and β = 107.663°). A spherical morphology was observed by scanning electron microscopy. The haemolytic activity carried out on human blood indicated that Ag-MnO nanocomposites are not toxic to human blood. Moreover, these particles showed a good antibacterial activity against gram-positive and gram-negative strains of bacteria. Promising results on the anthelmintic activity of Ag-MnO nanocomposites against several pathogenic helminths are reported in this paper. In addition to antibacterial and anthelmintic activities, Ag-MnO nanocomposites also exhibited good anti-inflammatory and antioxidant activities.

1. Introduction

Nanotechnology and nanoscience represent a new ‘world’ where matter has very different properties from what it has on a larger or macroscopic scale. Given their varied and often novel properties, bimetallic nanomaterials have diverse potentialities, and their uses open up multiple perspectives in many sectors of activity such as environment, health, automotive, construction, agri-food and electronics. Their properties are generally a synergistic combination of two metals which constitute them. Two approaches (bottom-up and top-down) are commonly used in the preparation of nanoparticles (NPs) [1-4].

In the top-down approach, we start from a large structure that is undersized, until reaching nanometric dimensions; in the bottom-up approach, the production of NPs is done by assembling atom by atom or molecule by molecule [5]. These two approaches use physical and chemical methods whose development for NP production on a large scale generally comes up against certain constraints, such as high energy consumption, low yield, use of harmful organic solvents as stabilisers, production of intermediates and generation of toxic waste at the base of environmental

* Corresponding author.
E-mail address: giresse.kasiama@unikin.ac.cd
DOI: 10.24237/djes.2023.16303

pollution. In addition, NPs produced by chemical methods keep the molecules used for stabilisation on their surfaces, thus limiting their uses in the medical and pharmaceutical fields because stabilisers define NPs' solubility and give them certain surface properties [6-8].

In this context, many studies are currently focused on the use of biological methods to produce NPs. Biological synthesis involves the use of extracts of living beings (e.g., plants and microorganisms) as reducing and stabilising agents; the first study carried out in this direction was the preparation of silver NPs using microorganisms [9]. Recent papers have reported the use of plant extracts in the preparation of metallic NPs.

Polyphenols (e.g., flavonoids and saponins), alkaloids, proteins, phenolic acids, sugars and terpenoids contained in various parts of plants play a key role in the reduction and stabilisation of metal ions to produce NPs. Thus, in addition to protecting the environment and human health by reducing the use of toxic chemicals, the utilisation of plant extracts reduces the number of steps, energy and preparation time, and NPs retain active chemical molecules on their surfaces, improving their efficacy and properties in the medical and pharmaceutical fields [10-12].

Amongst different types of metallic NPs, silver and manganese have attracted the attention of many researchers because of their multiple applications in various scientific fields. These NPs have been widely used as antibacterial, anthelmintic, antioxidant, optical, photovoltaic and photocatalytic agents [13-18].

However, no data exist on the association of these two metals in the form of nanocomposites using *Cyttaranthus congolensis* extract. This combination generally leads to the improvement of the properties of the material following a synergistic effect of their properties. Thus, this study is part of the search for a new material synthesised by green methods and having interesting biological properties.

In this study, Ag-MnO nanocomposites were synthesised using the aqueous extract of *C. congolensis* leaves. This plant is edible and belongs to the family of Euphorbiaceae. It is used as tea in traditional medicine to relieve sickle cell disease and is rich in polyphenolic and triterpenic compounds. It can play the role of reducer and stabiliser in Ag-MnO nanocomposite preparation. Several characterisation techniques were used to confirm the synthesis of these particles. Specifically, UV–visible (UV–vis) spectroscopy was adopted for surface plasmon resonance band, X-ray diffraction (XRD) analysis was used to study the crystal system and lattice parameters, and X-ray fluorescence analysis was utilised to assess the chemical composition. SEM was performed to determine particle morphology. The antibacterial activity of these nanocomposites was evaluated using diverse bacterial strains, such as *Escherichia coli*, *Staphylococcus aureus* and *Pseudomonas aeruginosa*.

2. Materials and methods

2.1.Materials

In this study, *C. congolensis* leaves were collected in Kwilu Province, Democratic Republic of the Congo. The plant was identified in the herbarium of the National Institute for Agronomic Studies and Research of the University of Kinshasa (UNIKIN). Five bacterial strains were used, including two gram-positive strains (*S. aureus* ATCC 25923, *S. aureus* ATCC 29213) and three gram-negative strains (*E. coli* ATCC 25922, *E. coli* ATCC 35 218 and *P. aeruginosa* ATCC 25783).

These strains were provided by the microbiology laboratory of the Faculty of Pharmaceutical Sciences of UNIKIN. The earthworm specimens were collected on the Keni River in Kinshasa. Manganese sulphate ($MnSO_4$), silver nitrate ($AgNO_3$) and resazurin were from Sigma-Aldrich. Cyanmethemoglobin (CMH) reagents and haemoglobin standards were purchased from StanBio. Two culture media, Mueller–Hinton agar (for the subculture of bacterial strains) and Mueller–Hinton broth (for the sensitivity test), were provided by the microbiology laboratory of the Faculty of Pharmaceutical Sciences of UNIKIN. Bidistilled water was used in the preparation of the solutions.

2.2.Chemical screening in solution and TLC

Fresh *C. congolensis* leaves were washed several times with water to remove impurities and dust, dried and then reduced to powder using a Sinbo-type grinder. Phytochemical screening of the solution was carried out following the procedure described by Ngoyi et al. [19]. A standard protocol based on spot colour observation was used for thin-layer chromatography to identify different secondary metabolites [20].

2.3. Assay of secondary metabolites

The total polyphenol content of the *C. congolensis* extract was determined using the Folin–Ciocalteu method [21]. The determination of total flavonoids and anthocyanins was carried out following the method described by Kasiama et al. [20].

2.4. Preparation of extracts

The *C. congolensis* powder (10 g) was macerated in 100 mL of bidistilled water for 24 h with stirring at room temperature. The aqueous extract was obtained after filtration with filter paper (Whatman No. 42) and stored in an airtight bottle at 6 °C.

2.5. Biosynthesis of Ag-MnO nanocomposites

The experimental procedure described by Kabengele was used for the biogenic synthesis of Ag-MnO nanocomposites [22].

The aqueous extract of *C. congolensis* was reacted with two equal concentrations of 0.1 N magnesium sulphate ($MnSO_4$) and 0.1 N silver nitrate ($AgNO_3$) solutions under thermal stirring at 60 °C and 1000 rpm. After 30 min of experiment, the colour change of the solution from yellow to dark brown showed the beginning of metal precipitation in the form of composite NPs. A few quantities of Ag-MnO NPs synthesised were kept for UV–vis spectroscopy. After 2 h of reaction, Ag-MnO was collected by centrifugation at 4000 rpm for 15 min, washed with distilled water, dried at 100 °C and stored for characterisation.

2.6. Characterisation of Ag-MnO nanocomposites

The synthesised Ag-MnO nanocomposites were characterised using various spectroscopic methods. UV–vis spectra were recorded using a Jenway 7315 UV–vis spectrophotometer. The particle morphology was determined using a TESCAN Lyra 3 scanning electron microscope. To determine the crystal structure and chemical composition of the nanocomposites, XRD patterns were obtained from an X-ray diffractometer (PHYWE 4.0) equipped with a CuKα radiation source ($\lambda = 1.5406$ Å) and an X-ray fluorescence spectrometer.

2.7. Antibacterial activity

The antibacterial activity was carried out via a microdilution method on a liquid medium (Mueller–Hinton medium) by using 96-well microplates [23].

2.8. Antioxidant activity

The antioxidant activity of the Ag-MnO nanocomposites was evaluated using DPPH test in accordance with the method used by Kasiama [20].

2.9. Anthelmintic activity

The anthelmintic activity of the Ag-MnO nanocomposites was evaluated in accordance with the method described by Kabengele [24].

2.10. Anti-inflammatory activity

In vitro anti-inflammatory activity was evaluated in accordance with the protein denaturation method (Albumin) described by Kumari [25].

2.11. Antihaemolytic activity

The test presented here is an adaptation of an existing standard, F-7560026, which is based on colorimetric detection of red-coloured CMH in a solution [26].

3. Results and discussion

3.1. Phytochemical screening and TLC

Various chemical groups were identified in *C. congolensis* leaves (polyphenols, alkaloids, triterpenoids and steroids), whereas saponins were absent. TLC images confirmed the presence of triterpenes, anthracene derivatives, flavonoids, alkaloids and coumarins, as presented in the figures below.

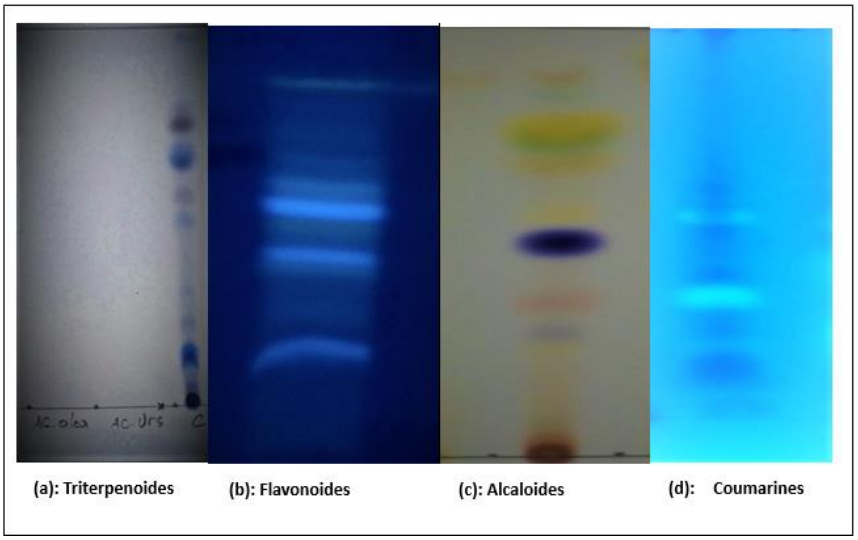

Figure 1. CCM images of triterpenoids (a), Flavonoids (b), Alcaloids (c) Coumarins (d)

Figure 1a depicts the spots corresponding to triterpenoids in *C. congolensis*, revealed by brown-coloured spots after development with sulphuric acid–anisaldehyde and heating for 10 min. The chromatogram in Figure 1b confirmed the presence of flavonoids by blue spots after development under a UV lamp. The presence of alkaloids was revealed by yellow-coloured spots after revelation with 5% sodium nitrite solution, as shown in Figure 1c. The coumarins on chromatoplate in Figure 1d showed blue- and purple-coloured spots after spraying 10% ethanolic KOH and observing at 366 nm.

3.2. Secondary metabolite content

3.2.1. Polyphenol content

Table 1 presents the contents of total polyphenols, flavonoids, anthocyanins and condensed and hydrolysable tannins in *C. congolensis* leaves.

Table 1: Content of total polyphenols, flavonoids, anthocyanins, condensed tannins and hydrolysable tannins in *C. congolensis*

Plants	Secondary metabolites				
	Total polyphenols (µg EAG /g)	**Flavonoids (%)**	**Anthocyanins (%)**	**Condensed tannins (%)**	**Hydrolysable tannins (%)**
C. congolensis	458.220 ± 7.50	4.136±0.002	2.253 ± 0.004	3.431 ± 0.009	5.529 ± 0.005

The determination of total polyphenols, flavonoids, tannins and anthocyanins was carried out by UV–vis spectrophotometry. The results obtained showed high levels of total polyphenols (flavonoids and tannins).

3.3. Synthesis

The reaction medium changed from a pale-yellow colour to a brown colour after 30 min, as shown in Figure 2. This colour change was due to the excitation of surface plasmon vibrations in Ag-MnO nanocomposites [27].

Figure 2. Formation of nanoparticles in solution

3.4.Characterisation of nanocomposites

3.4.1. UV–vis spectroscopy of nanocomposites

The presence of Ag-MnO nanocomposites in the solution was confirmed by UV–vis spectral analysis after 2 h of contact, as presented in Figure 3. A broad peak located between 350 and 400 nm, attributed to Ag-MnO NPs, was observed. This peak was related to surface plasmon resonance, which has already been well documented for various metallic NPs with sizes ranging from 2 nm to 100 nm [28].

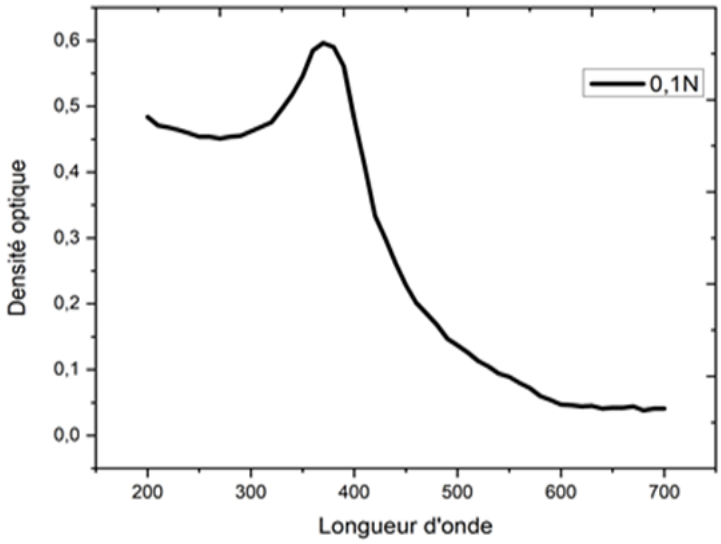

Figure 3. UV-visible spectrum of Ag -MnO nanocomposites

3.4.2. Chemical composition of nanocomposites

XRD studies of synthesised nanocomposites were performed at room temperature with a 4.0 PHYWE diffractometer using a Cu Kα radiation source. Figure 4 and Table 2 show the XRD spectrum and its summary.

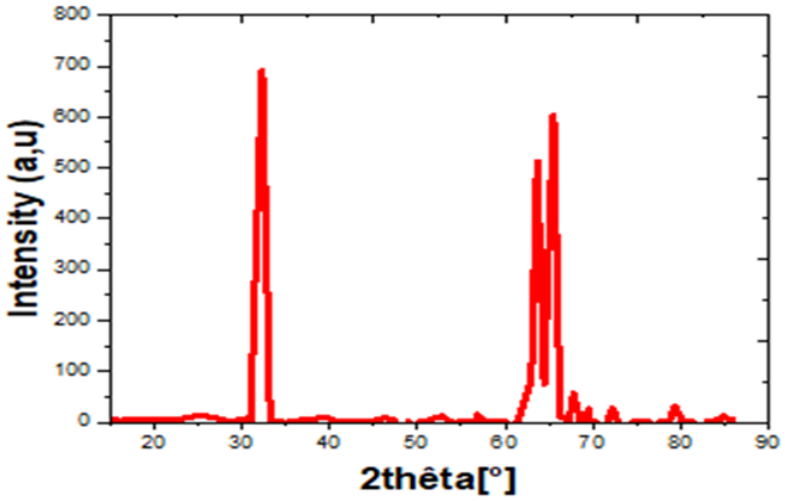

Figure 4. XRD diagram of synthesized Ag-MnO nanocomposites

Table 2: XRD peak values of Ag-MnO nanocomposites

No.	**2 thetas**[°]	[***A***]	I/I_0	**Accounts (peak area)**	**FWHM**
6	30.48	2.9300	904.12	3.83	1.3292
8	33.19	2.6971	972.91	1.12	0.3625
27	63.67	1.4604	455.74	2.05	1.4121
28	65.53	1.4234	556.67	2.39	1.3453

Table 2 presents four characteristic 2 theta peaks of Ag-MnO nanocomposites. The composition of these particles was Ag 0.21 Mn 0.28 O which crystallised in a monoclinic system having the following lattice parameters: a = 5.8517 A, b = 3.4674 A, c = 5.4838 and β = 107.663°. The calculated density was ϕ = 7.760 g/cm^3. The average size determined via the Debye–Scherrer equation was d = (kλ/βcosθ), where k is the Debye–Scherrer constant (0.89), λ is the wavelength of the X-ray (0.154 nm), β is the width of the maximum intensity peak at mid-height, d is the crystal thickness, and θ is the diffraction angle [29-31]. After calculation, the average size of the crystallites of the particles was 9.75 nm. The X-ray fluorescence spectrum in Figure 5 allowed us to identify the presence of the metals silver (Ag-Kα and Ag-Kβ) and manganese (Mn-Kα and Mn-Kβ).

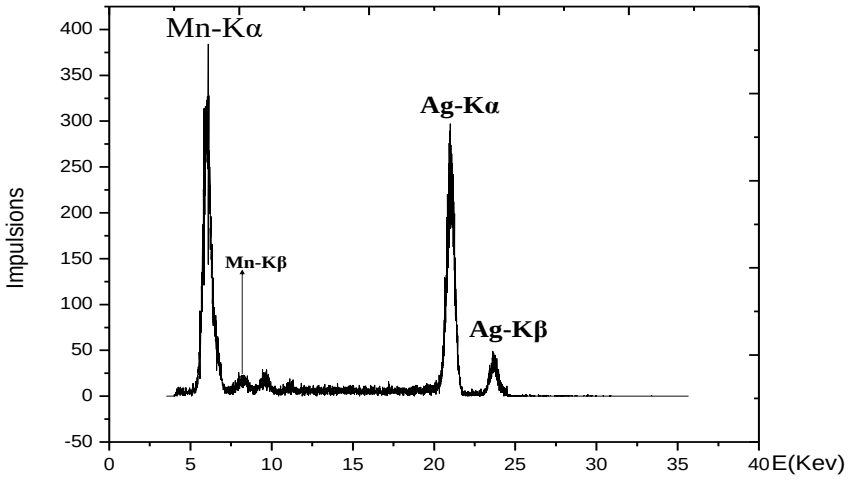

Figure 5. X-ray fluorescence spectrum of Ag-MnO nanoparticles

3.4.3. Morphology of nanocomposites

The morphology of the synthesised Ag-MnO nanocomposites was determined by scanning electron microscopy (SEM). SEM images of Ag-MnO nanocomposites are shown in Figure 6.

Predominant spherical shapes were observed. A similar morphology has been reported in previous work [32].

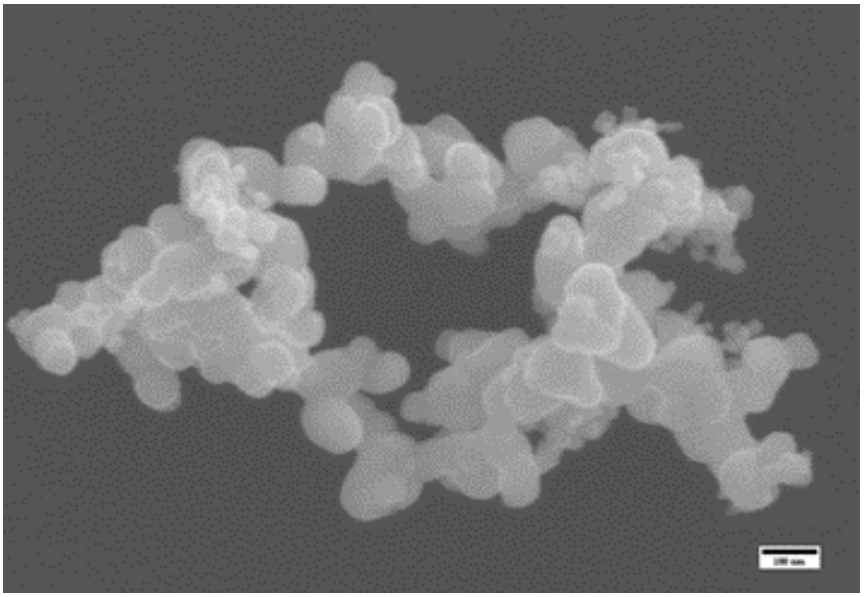

Figure 6. Morphology of Ag-MnO nanoparticles

3.5. Antibacterial activity

The results indicated that the antibacterial effect was proportional to the concentration of the Ag-MnO nanocomposites used. The growth inhibition of *E. coli* strains by different concentrations of Ag-MnONPs was greater than that of the other bacteria tested. Minimum inhibitory concentrations (MIC) were obtained at 31.25 µg/mL for *E. coli* ATCC 25922 and 62.5 µg/mL for *E. coli* ATCC 35 218. For *S. aureus* strains (*S. aureus* ATCC 25923 and *S. aureus* ATCC 29213), the MIC was equal to 125 µg/mL. For *P. aeruginosa* ATCC 25783, Ag-

MnO NPs inhibited their development at MIC of 125 µg/mL. With ciprofloxacin, which was considered the reference antibiotic, a total inhibition of bacterial growth was observed for MIC of 0.25 µg/mL. The Ag-MnO NPs exerted a bactericidal effect on all strains used in this study, see Table 3.

The mechanism of action of Ag-MnO NPs came from the electron pairs created on the surface of Ag-MnO NPs, which influenced the oxidation–reduction reaction capable to generate reactive oxygen species (ROS). In the presence of these free radicals, microorganisms' cells will be immediately destroyed via peptidoglycan and cell membranes, DNA, mRNA, ribosomes and proteins. Another mechanism has been proposed, in which the bactericidal effect of NPs is mainly explained by the rupture of the lipid double layer of bacteria, resulting in the leakage of cytoplasmic content [33,34].

Table 3: Different concentrations of Ag-MnO NPs tested on gram+ and gram- bacteria

Bacteria	**Concentrations (µg/mL) of Ag-MnONPs**											
	T+	T-	3.90625	7.8125	15,625	31.25	62.5	125	250	500	1000	2000
S. aureus ATCC 29213	-	+	+	+	+	+	+	-	-	-	-	-
E. coli ATCC 35 218	-	+	+	+	+	+	-	-	-	-	-	-
P. aeruginosa ATCC 25783	-	+	+	+	+	+	+	-	-	-	-	-
S. aureus ATCC 29213	-	+	+	+	+	+	+	-	-	-	-	-
E. coli ATCC 25922	-	+	+	+	+	-	-	-	-	-	-	-

Legend: +: growth of bacteria
-: no growth of bacteria

3.6. Anthelmintic activity

Figure 7 gives the paralysis time of worms as a function of nanocomposite concentration.

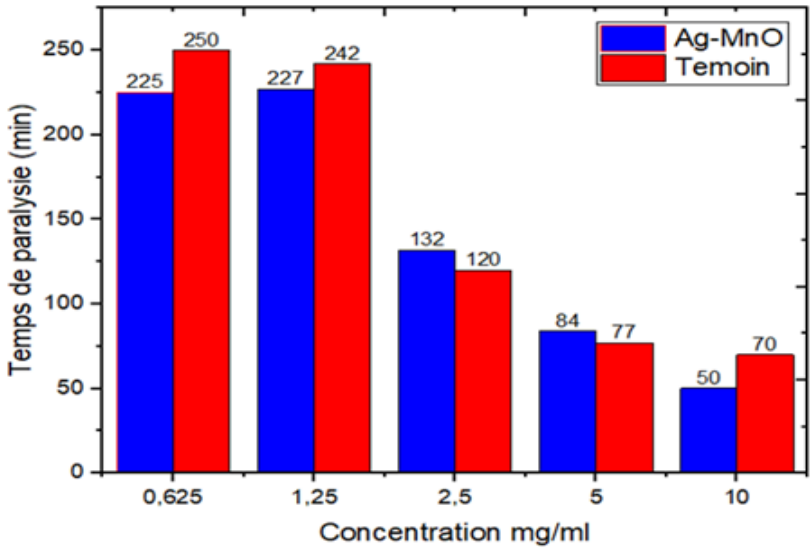

Figure 7. Paralysis time of worms as a function of drug concentration.

The worm paralysis time decreased when the concentration of Ag-MnO nanocomposites increased (from 0.625 mg/mL to 10 mg/mL). At a high dose (10 mg/mL), this time decreased approximately 4–5 times, depending on the case.

Figure 8 gives the earthworm mortality rate as a function of the concentration of Ag-MnO nanocomposites.

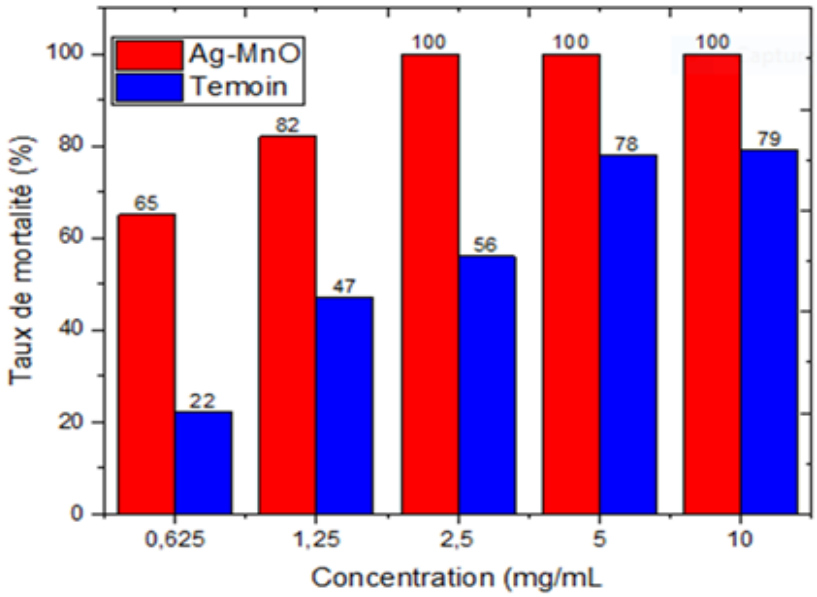

Figure 8. Worm mortality rate as a function of Ag-MnO nanocomposite concentration

The mortality rate of worms was dose-dependent, i.e., it increased with the concentration. Ag-MnO nanocomposites were more active than the mebendazole used as a positive control. The anthelmintic activity of the Ag-MnO nanocomposites was due to their capacity to create ROS in a medium [33].

3.7. Antioxidant activity

Figure 9 illustrates the evolution of the inhibition rate of DPPH radicals.

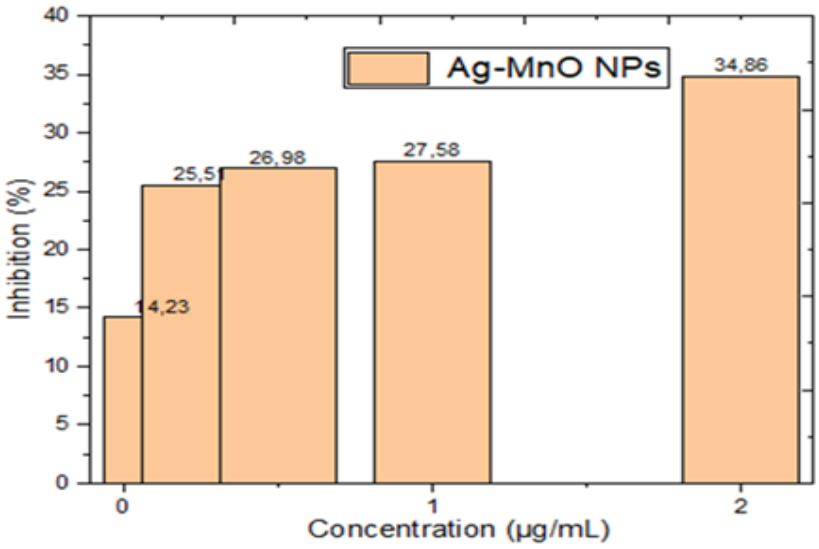

Figure 9. Inhibition rate of the DPPH radical by Ag-MnO nanocomposites.

The inhibition rate of DPPH radicals was dose-dependent. DPPH, a purple-coloured free radical, was reduced to a yellow-coloured compound in the presence of scavenging compounds. The antioxidant activity of the Ag-MnO nanocomposites was due to the presence of secondary plant metabolites, which served for stabilisation during the formation of these nanocomposites [35].

3.8. Anti-inflammatory activity

The anti-inflammatory effect of the nanocomposites was assessed in vitro against protein denaturation. Figure 10 gives the rate of inhibition of the thermal denaturation of ovalbumin in vitro (%I) of the Ag-MnO nanocomposites.

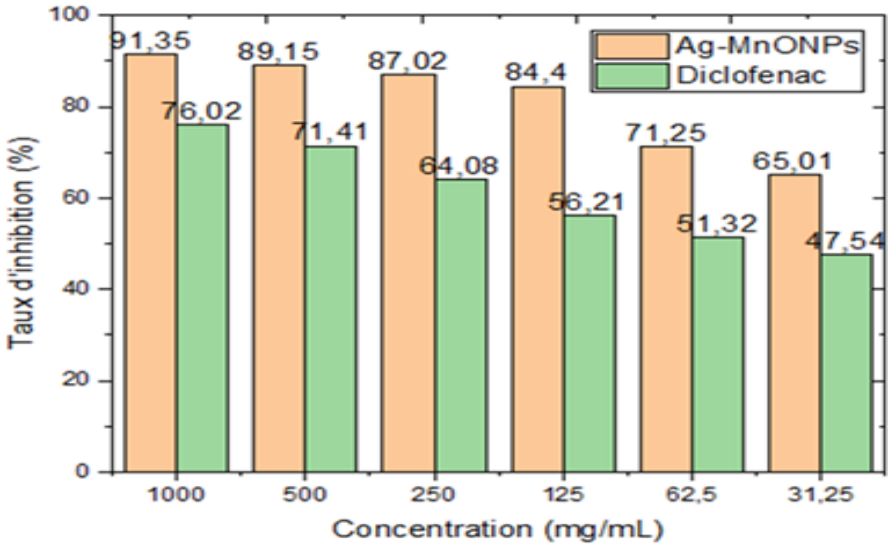

Figure 10. Percentage inhibition of protein denaturation (albumin)

The results indicated the concentration-dependent inhibition of protein denaturation by Ag-MnO nanocomposites. In Figure 10, the Ag-MnO nanocomposites exhibited an anti-inflammatory activity. The ovalbumin thermal denaturation inhibition rates were 65.01%, 71.25%, 84.4%, 87.02%, 89.15% and 91.35% for the Ag-MnO nanocomposites at doses of 62.5, 31.25, 125, 250, 500 and 1000 mg/mL, respectively. Diclofenac sodium at the same doses as Ag-MnO NPs was used as a reference molecule, and the percentages of inhibition were 47.54%, 51.32%, 56.21%, 64.08%, 71.41% and 76.02%. These results showed that the anti-inflammatory effect of the Ag-MnO nanocomposites was superior to that of diclofenac. Thus, the work of Jain and Priyanka based on silver NPs reported an appreciable but lower anti-inflammatory effect compared with those proven by Ag-MnO nanocomposites. This result might be due to the combination of manganese, which implied an additive effect [36,37].

3.9. Cytotoxicity

Cytotoxicity was assessed using erythrocytes as a biological model. The extract was considered cytotoxic when, at 10 µg/mL, the haemolysis rate was ≥ 50%. This study determined that the Ag-MnO nanocomposites were minimally haemolytic (% haemolysis = 6.49 1.089). However, at 100 µg/mL, the homolysis rate was less than 50%, which showed that the Ag-MnO nanocomposites had no effect on haemolysis and could be used therapeutically.

4. Conclusions

The objectives of this study were to synthesise Ag-MnO nanocomposites from silver nitrate and manganese sulphate salts using the aqueous extract of *C. congolensis* leaves and to evaluate their biological activities (antibacterial, anthelmintic, antioxidant, anti-inflammatory and haemolytic). *C. congolensis* presented a good phytochemical profile and thin-layer chromatography. An assay of secondary metabolites capable of reducing and stabilising metals in NPs was also conducted.

These biosynthesised nanocomposites were characterised using several spectroscopic methods and exhibited good antibacterial, anti-inflammatory, anthelmintic and antioxidant properties. They are nonhaemotoxic. This

finding confirmed their potential to be used in therapy. In consideration of the negative impact of conventional NP synthesis methods, green synthesis is the best alternative for the synthesis of minimally toxic NPs. This research led to the development of a new cost-effective synthetic strategy and the reduction of chemical use in further studies. Some points remain to be further investigated, and certain biological tests may be carried out to exploit other biological potentials of these new Ag-MnO materials.

References

[1] T. Dodevska, I. Vasileva, P. Denev, D. Karashanova, B. Georgieva, D. Kovacheva, N. Yantcheva, A. Slavov, R. damascene. waste mediated synthesis of silver nanoparticles: Characteristics and application for an electrochemical sensing of hydrogen peroxide and vanillin, Materials Chemistry and Physics.; 231(2019)335-343. https://doi.org/10.1016/j.matchemphys.2019.04.030 .

[2] N. Ahmad, F. indéfini, M. Jabeen, Z. Ul Haq, I. Ahmad, A. Wahab, Z.U. Islam, R. Ullah, A. Bari, M.A. Mohamed, F.M. El-Demerdash, M.K. Yahya. "Green Manufacture of silver nanoparticles using the aqueous extract of Euphorbia serpens Kunth, their characterization and the study of its antioxidant, antimicrobial, insecticidal and cytotoxic activities in vitro", BioMed Research International. 5562849 (2022) 11. https://doi.org/10.1155/2022/5562849.

[3] M. Ovais, A.T. Khalil, A. Raza, M.A. Khan, I. Ahmad, N.U. Islam, M. Saravanan, M.F. Ubaid, M. Ali, Z.K. Shinwari. Green synthesis of silver nanoparticles via plant extracts: beginning a new era in cancer theranostics. Nanomedicine (Lond). 11 (2016) 3157-3177. doi: 10.2217/nnm-2016-0279.

[4] Z. Fereshteh, M.R.L. Estarki, R.S. Razavi, M. Taheran. Template synthesis of zinc oxide nanoparticles entrapped in the zeolite Y matrix and applying them for thermal control paint, Materials Science in Semiconductor Processing. 16 (2013) 547-553. https://doi.org/10.1016/j.mssp.2012.08.005.

[5] Z.U.H. Khan, A. Khan, Y. Chen, N.S. Shah, N. Muhammad, A.U. Khan, K. Tahir, F.U. Khan, B. Murtaza, S.U. Hassan, S.A. Qaisrani, P. Wan. Biomedical applications of green synthesized Nobel metal nanoparticles, Journal of Photochemistry and Photobiology B: Biology. 173 (2017) 150-164. https://doi.org/10.1016/j.jphotobiol.2017.05.034.

[6] M. Rafique, I. Sadaf, M.S. Rafique, M.B. Tahir. A review on green synthesis of silver nanoparticles and their applications. Artif Cells Nanomed Biotechnol. 45 (2017) 1272-1291. doi: 10.1080/21691401.2016.1241792.

[7] A. Happy, M. Soumya, S.V. Kumar, S. Rajeshkumar, R.D. Sheba, T. Lakshmi, V.D. Nallaswamy. Phyto-assisted synthesis of zinc oxide nanoparticles using Cassia alata and its antibacterial activity against Escherichia coli, Biochemistry and Biophysics Reports. 17 (2019) 208-211. https://doi.org/10.1016/j.bbrep.2019.01.002.

[8] M. Herlekar, S. Barve, R. Kumar. "Synthèse verte médiée par les plantes de nanoparticules de fer", Journal of Nanoparticles. 9 (2014) 140614. https://doi.org/10.1155/2014/140614

[9] S. Ahmed, M. Ahmad, B.L. Swami, S. Ikram. A review on plants extracts mediated synthesis of silver nanoparticles for antimicrobial applications: A green expertise. J Adv Res. 7 (2016) 17-28. doi: 10.1016/j.jare.2015.02.007.

[10] G.K. Prashanth, P.A. Prashanth, U. Bora, M. Gadewar, B.M. Nagabhushana, S. Ananda, G.M. Krishnaiah, H.M. Sathyananda. In vitro antibacterial and cytotoxicity studies of ZnO nanopowders prepared by combustion assisted facile green synthesis, Karbala International Journal of Modern Science.1(2015) 67-77. https://doi.org/10.1016/j.kijoms.2015.10.007.

[11] M. Harshiny, M. Matheswaran, G. Arthanareeswaran, S. Kumaran, S. Rajasree. Enhancement of antibacterial properties of silver nanoparticles–ceftriaxone conjugate through Mukia maderaspatana leaf extract mediated synthesis, Ecotoxicology and Environmental Safety. 121(2015)135-141. https://doi.org/10.1016/j.ecoenv.2015.04.041.

[12] D.I. Pantelis, P.N. Karakizis, N.M. Daniolos, C.A. Charitidis, E.P. Koumoulos and D.A. Dragatogiannis. Microstructural study and mechanical properties of dissimilar AA5083-H111 and AA6082-T6 friction welds reinforced with SiC nanoparticles, materials and fabrication processes. 31 (2016) 264-274, DOI: 10.1080/10426914.2015.1019095

[13] T. Zohra, A.T. Khalil, F. Saeed, B. Latif, M. Salman, A. Ikram, M. Ayaz, H.C.A. Murthy. "Green Nano-Biotechnology: A New Sustainable Paradigm to Control Dengue Infection", Bioinorganic Chemistry and Applications. 3994340 (2022) 21. https://doi.org/10.1155/2022/3994340

[14] C.E. Lemaoui, H. Layaida, A. Badi, N. Foudi. Stratégies actuelles de lutte contre la résistance aux antibiotiques, Journal des Anti-infectieux. 19(2017)12-19. https://doi.org/10.1016/j.antinf.2017.01.003.

[15] D. Floresyona. Synthesis of Metal and Conjugated Polymer Nanostructures in Hexagonal Mesophases for Application in Fuel Cells and photocatalysis. Polymers. Paris Saclay University (COmUE). (2017). English. ⟨NNT: 2017SACLS206⟩. ⟨tel-01865813⟩

[16] J. Sourice. Synthesis of core-shell silicon-carbon nanocomposites by double-stage laser pyrolysis: application to the anode of lithium-ion batteries. Materials. Paris Sud University - Paris XI. (2015). French. ⟨NNT: 2015PA112166⟩. ⟨tel-01302856⟩

[17] N.M. El Fatah. Fabrication and characterization of Ag@AgCl nanocomposite thin films for photovoltaic applications. (2021). Doctoral thesis. http://hdl.handle.net/123456789/3350

[18] J.G. Mattei. Structure and chemical order in bimetallic nanoparticles: case of the Fe-Bi immiscible system. Materials Science [cond-mat.mtrl-sci]. Paul Sabatier University (Toulouse 3). (2012). French. ⟨NNT: 2012TOU30302⟩. ⟨tel-01937619⟩.

[19] E.M. Ngoyi, D.D. Tshilanda, J.T. Kilembe, E.M. Lengbiye, C.N. Kabengele, G.N. Kasiama, D.T.S. Tshibangu, D.O. Opota, K. Ngbolua, P.T. Mpiana. Phytochemical profile, antioxidant and anthelmintic activities of O. gratissimum leaves collected in Kinshasa (D.R. Congo). Discovery Phytomedicine.; 7(2020) 171-176. DOI: 10.15562/phytomedicine.

[20] G.N. Kasiama, A. Ikey, C.N. Kabengele, J.T. Kilembe, E.N. Matshimba, J.M. Bete, P.B. Bahati, C.L. Inkoto, P.K. Mutwale, K.N. Ngbolua, D.S.T. Tshibangu, D.D. Tshilanda and P.T. Mpiana*. Anthelmintic activity, antioxidant activity, phytochemical profile and microscopic features of Cassia alata collected in the Democratic Republic of Congo (DR Congo). 37(2022) 28-36; Article no.ARRB .87349. DOI: 10.9734/ARRB/2022/v37i630513

[21] K. Ngombe, F. Bukatuta, M. Kapepula, B. Moni, K. Makengo, L. Pambu, N. Bongo, M. Mbombo, M. Musuyu, U. Maloueki, N. Koto-Te-Nyiwa and F. Mbemba. Bioactivity and Nutritional values of some Dioscorea species traditionally used as Medicinal foods in Bandundu, DR congo, EJMP. 14(2016) 1-11, DOI: 10.9734/EJMP/2016/25124

[22] C.N. Kabengele, G.N .Kasiama, E.M. Ngoyi, C.L. Inkoto, J.M. Bete, P.B. Babady, D.S.T. Tshibangu, D.D. Tshilanda, H.M. Kalele, P.T. Mpiana, K. Ngbolua. Biogenic synthesis, characterization and effects of Mn-CuO composite nanocatalysts on Methylene blue photodegradation and Human erythrocytes[J]. AIMS Materials Science. 10(2023)356-369. doi: 10.3934/matersci.2023019

[23] S. Hatakeyama, Y. Ohama, M. Okazaki, Y. Nukui & K. Moriya. Test de sensibilité aux antimicrobiens de mycobactéries à croissance rapide isolées au Japon. BMC Infect Dis. 17 (2017).197. https://doi.org/10.1186/s12879-017-2298-8.

[24] C.N. Kabengele, E. M.Ngoyi, G.N. Kasiama, J.T. Kilembe, A. Matondo, C.L. Inkoto, E.M. Lengbiye, C.M. Mbadiko, J.J.D. Amogu, G.N. Bongo … P.T. Mpiana. Antihelminthic Activity, Phytochemical Profile and Microscopic Features of Ocimum basilicum Collected in DR Congo. AJOB. 10(2020) 42-50. DOI: 10.9734/AJOB/2020/v10i330110

[25] K.C. Sree, N. Yasmin, R.M. Hussain and M. Babuselvam. Invitro anti-inflammatory and anti-arthritic property of rhizopora mucronata leaves. International Journal of Pharma Sciences and Research (IJPSR). Flight.; 6 (2015) 3. ISSN: 0975-9492.

[26] A. Marina, D. Jeffrey, W. Barry, B. Jennifer, K. Anil and E. Scott. Method for Analysis of Nanoparticle Hemolytic Properties In Vitro. Nano Lett. 8(2009) 2180–2187. doi:10.1021/nl0805615.

[27] J.Y. Song et B.S. Kim. Synthèse biologique rapide de nanoparticules d'argent à l'aide d'extraits de feuilles de plantes. Bioprocess Biosyst Eng. 32(2009)79–84. https://doi.org/10.1007/s00449-008-0224-6

[28] S. Iravani. "Bacteria in Nanoparticle Synthesis: Current Status and Future Prospects", International Scholarly Research Notices. 18(2014) 359316. https://doi.org/10.1155/2014/359316

[29] M. Souri, V. Hoseinpour, N. Ghaemi and A. Shakeri. Optimisation de la procédure pour la synthèse verte de nanoparticules de dioxyde de manganèse par l'extrait de feuille de Yucca gloriosa. Int Nano Lett. 9(2019) 73–81. https://doi.org/10.1007/s40089-018-0257-z

[30] A. Khataee, M. Sheydaei, A. Hassani, M. Taseidifar and S. Karaca. Sonocatalytic removal of an organic dye using TiO2/montmoril lonite nanocomposite. Ultrasound. Sonochem. 22(2015)404–411. https://doi.org/10.1016/j.ultsonch.2014.07.002.

[31] Z. Alhalili. Green synthesis of copper oxide nanoparticles CuO NPs from Eucalyptus Globoulus leaf extract: Adsorption and design of experiments, Arabian Journal of Chemistry. 15(2022)1878-5352. https://doi.org/10.1016/j.arabjc.2022.103739.

[32] A. Nawaz, S. Bano, M. Yasir, A. Wadood and M.A. Rehman. Ag and Mn-doped mesoporous bioactive glass nanoparticles incorporated into the chitosan/ gelatin coatings deposited on PEEK/bioactive glass layers for favorable osteogenic differentiation and antibacterial activity. Mater. Adv. 1(2020) 1273-1284. DOI: 10.1039/d0ma00325e.

[33] H. Xu. Elaboration of laccase T. cross-linked ultraporous aluminas for Remazol Brilliant Blue R

removal. Material chemistry. Université Paris-Nord - Paris XIII. (2021) English. ⟨NNT: 2021PA131076⟩. ⟨tel-03886067⟩

[34] M.H. Yap, K.L. Fow, G.Z. Chen. Synthesis and applications of MOF-derived porous nanostructures, Green Energy & Environment.; 2(2017)218-245. https://doi.org/10.1016/j.gee.2017.05.003.

[35] M.H. El-Rafie and M.A. Hamed. Antioxidant and anti-inflammatory activities of silver nanoparticles biosynthesized from aqueous leaves extracts of four Terminalia species. Adv. Nat. Sci: Nanosci. Nanotechnology.; 5(2014)035008. DOI 10.1088/2043-6262/5/3/035008.

[36] J. Aditya, A. Roy, S. Rajeshkumar. Anti-inflammatory activity of silver nanoparticles synthesized using cumin oil. Research Journal of Pharmacy and Technology.); 12(2019)2790-2793; DOI: 10.5958/0974-360X.2019.00469.4

[37] P. Singh, S. Ahn, J.P. Kang, S. Veronika, Y. Huo, H. Singh, M. Chokkaligam, F.M. Agamy, V.C. Aceituno, Y.J. Kim, D.C. Yang. In vitro anti-inflammatory activity of spherical silver nanoparticles and monodisperse hexagonal gold nanoparticles by fruit extract of Prunus serrulata: a green synthetic approach. Artif Cells Nanomed Biotechnol. 46(2018)2022-2032. doi: 10.1080/21691401.2017.1408117.